

UCSD-SP-66-3

DISTORTION OF THE MAGNETOSPHERE

DURING A MAGNETIC STORM ON 30 SEPTEMBER, 1961

GPO PRICE \$ _____

CFSTI PRICE(S) \$ _____

Hard copy (HC) 2.00

Microfilm (MF) .50

653 July 65

L. J. Cahill, Jr.

University of California, San Diego

La Jolla, California

and

D. H. Bailey

University of New Hampshire

Durham, New Hampshire

June 1966

30846
(TITLE)
1
(CODE)
29
(CATEGORY)
N66
(ACCESSION NUMBER)
37
(PAGES)
CR-76362
(NASA CR OR TMX OR AD NUMBER)

Abstract

30846

A sudden commencement magnetic storm started on 30 September, 1961. The Explorer 12 Satellite was in orbit, in the day side of the magnetosphere, during the storm. During the recovery phase of the storm the field magnitude at 4 earth radii, and at magnetic latitudes above 20° , was increased. A low latitude pass, late in the recovery phase, revealed a field depression at 4 R_e near the equator. The field distortions observed are attributed to inflation of the magnetosphere by low energy charged particles on field lines from $L = 2$ to $L = 5$.

Author

Distortion of the Magnetosphere
During a Magnetic Storm on 30 September, 1961

L. J. Cahill, Jr.

University of California, San Diego

and

D. H. Bailey

University of New Hampshire

Introduction

The main phase of a magnetic storm is recognized as a world-wide depression of the horizontal component of the earth's magnetic field. The sudden commencement and initial phase of a storm were attributed by Chapman and Ferraro (1931) to compression of the earth's magnetic field by a stream of plasma from the sun. They also proposed that the main phase was caused by entry of some of the plasma into a cavity formed as the plasma flowed around the earth's magnetic field (Chapman and Ferraro, 1933). According to them, captured plasma formed a ring current flowing around the earth at a distance of several earth radii from the earth's center. The decay of the main phase magnetic field depression, lasting for several days, was interpreted as a gradual decrease in intensity of the ring current.

Singer (1957) first proposed that the motions of charged particles trapped in the geomagnetic field could produce a ring current. The discovery of the trapped particle belts by Van Allen (1959) gave impetus to this concept. Detailed calculations of the magnetic field contributions

of trapped particles have been presented (Dessler and Parker, 1959; Dessler, Hanson and Parker, 1961; Akasofu and Chapman, 1961; Akasofu, Cain and Chapman, 1961, 1962; Apel, Singer and Wentworth, 1962; Kern, 1962; Beard, 1962). The helical motions of particles along the magnetic lines of force and the drift motion in longitude, when considered in detail, can be considered as a net electrical current. This current produces a depression of the magnetic field at the region of high particle flux and at lower altitudes; it produces an increase in field strength at higher altitudes.

With the advent of satellite experiments in the magnetosphere, an early discovery of the ring current was anticipated. Magnetic field experiments were included on satellites as early as 1958, and charged particle detectors were flown that could, hopefully, reveal the ring current particles. Although the size and shape of the magnetosphere have been determined and the charged particle populations over a wide range of energies have been studied, the location of the ring current and identification of the particles responsible for it are still uncertain.

The Russian Lunik 1 and Lunik 2 space probes observed, in 1959, a field depression near 3 earth radii (R_e) that could be interpreted as due to a ring current (Dolginov et al., 1961). Vanguard 3 provided precise, though low-altitude, field magnitude measurements that indicated the ring current must be above $1.1 R_e$ (Cain et al., 1962). Explorer 6 measurements of one field component (in a plane perpendicular to the vehicle spin axis) showed a depression near 7 earth radii on the dark side of the magnetosphere (Smith, 1962). Explorer 10 measurements suggested a field depression below $4 R_e$ (Heppner et al., 1963). Explorer 12

measurements indicated that there were no substantial depressions of the field above $5 R_e$ in the sunlit hemisphere (Cahill and Amazeen, 1963; Cahill and Patel, 1966). During the magnetic storm of 30 September, 1961, the magnetosphere field magnitude was observed to rise near $4 R_e$ (Patel and Cahill, 1962; Cahill and Bailey, 1965). Explorer 14 measurements in the dark hemisphere in 1963 showed a field depression near $8 R_e$ that may be similar to that observed by Explorer 6 (Cahill, 1966). This has been interpreted, however, as due principally to inflation of the geomagnetic field by particles outside the "durable" trapping region, probably the near-earth portion of the neutral sheet observed by Ness (1965) in the magnetosphere tail. Elektron 2, a high-inclination Russian satellite, has provided magnetic measurements in the dark hemisphere that show a field depression commencing between 5 and $7 R_e$ and extending inward with increasing magnitude to at least $3 R_e$ (Dolginov et al., 1966).

The search for charged particles of sufficient energy density to produce a significant ring current has been largely unsuccessful. The more energetic particles (protons of energy > 1 Mev and electrons of energy > 50 kev), observed to date, have insufficient flux, by several orders of magnitude, to produce measurable magnetic effects at the earth's surface. Measurements by Davis and Williamson (1963) indicated that protons of energies greater than 100 kev, located near $3 R_e$, possess energy density sufficient to produce a small, but measurable, field depression (Hoffman and Bracken, 1965). Electrons of energy greater than 10 kev, measured in the same experiment, were too low in energy density by several orders of magnitude. Frank, 1966 has recently reported observation of low energy electrons by the Cadmium Sulphide total energy detector on Explorer 12. The energy of these electrons cannot be specified uniquely, but if an average energy of 1 kev

is assumed, a substantial field depression would result.

Parker (1962) and Akasofu (1963) have recently reviewed experimental and theoretical studies of magnetic storms. It appears that a ring current that can produce a surface depression of 100 gammas must lie quite close to the earth, 2 to 4 R_e . Although a given energy density of particles causes a greater depression of the field when distributed over a more distant L shell, the maximum depression is limited by the local strength of the main field. At 7 earth radii the main field is only 100 gammas and can not support a belt of particles producing a 100-gamma depression at earth. It is probable that the ring current belt consists primarily of protons, $E < 100$ kev, but electrons, $E < 10$ kev, may also contribute to the field depression.

Akasofu, Chapman and Venkatesan (1963) pointed out two distinct portions of the main phase of large storms, one in which the maximum depression occurs and for which recovery is rapid, and a second phase for which the recovery takes several days. They have suggested that there may be two different belts responsible for this behavior, perhaps located in different regions of the magnetosphere.

In the present paper the experimental evidence for ring currents obtained from the Explorer 12 satellite will be critically examined for the region of the magnetosphere between 3 R_e and the boundary. In particular, the data obtained during a large magnetic storm, on 30 September, 1961, will be presented and compared with results from more quiet periods.

Experiment

The magnetometer experiment and the satellite orbit have been described in earlier papers (Cahill and Amazeen, 1963; Cahill and Patel, 1966). The use of the data for investigation of ring current effects demands some additional discussion of errors. In the boundary studies the perturbations in the field magnitude were comparable to the predicted field. In the present study the perturbations we are looking for are a very small fraction of the total field. The principal sources of error are digitization (± 12 gammas for each of three perpendicular sensors for each individual measurement), zero level drift (estimated to be less than 10 gammas for each sensor), and change in sensitivity of the magnetometers (change in slope of the calibration curve after preflight calibration). The effects of digitization error can usually be made quite small by averaging many data points. The zero level drift is of concern when measuring small fields beyond the magnetopause. For field magnitudes of several hundred gammas a possible zero level error of 10 gammas is less important although it cannot be neglected. Any change in calibration slope becomes more important at high field magnitudes.

Fortunately the magnetometer design provides for great stability against change in sensitivity. Most of the factors that might change sensitivity would produce a much larger change in zero level; absence of significant change in zero level has been noted. An in-flight calibration sequence allows a check of magnetometer sensitivity. We estimate that the slopes of the component magnetometer calibration curves have not changed as much as 1% (10 gammas at full scale, 1000 gammas) during the period to be analyzed. The maximum error, due to calibration change, in a single measurement of field magnitude at a level of 1000 gammas at

$3 R_e$ is therefore lower than 10 gammas. At $5 R_e$ where the field is 300 γ , this error is less than 3 gammas. Error due to a change in space craft magnetic field after preflight calibration is estimated to be less than 10 gammas.

In order to compare measured and predicted field directions, it is necessary to transform from satellite coordinates (B , α , and ψ) to accurate geomagnetic dipole components B_r , B_θ , and B_ϕ . This requires accurate knowledge of the direction of the satellite spin axis in inertial space. Although this direction has been determined, from solar aspect data, to an accuracy of a few degrees, there is still some uncertainty about direction. When the field magnitude is 1000 gammas, a few degrees error will produce a large error in field components. For this reason we have chosen, at present, to compare only field magnitude.

Finally, in the results to be presented we will rely mainly on changes in field magnitude from one pass to the next. Changes in field magnitude will be shown on successive passes in a similar region of space; these changes are apparently caused by a large magnetic storm.

Results

The magnetic storm index, Dst, is shown in Figure 1 for a 17 day period including the 30 September storm. The outbound pass immediately preceding the storm sudden commencement is shown in Figure 2. The boundary is seen at $10.4 R_e$. This boundary penetration was somewhat unusual, however, since it was identified as associated with a world wide positive sudden impulse (Nishida and Cahill, 1964). The boundary apparently moved in past the satellite just after the beginning of the sudden impulse at the satellite. This sudden impulse occurred 2 hrs. 18 min. before the sudden commencement at 2108 UT. Figure 3 shows 2 hours of data including the sudden commencement time. Charged particle measurements from Explorer 12, at this time, have been previously reported (Hoffman et al, 1962; Bryant et al, 1962). A drop in field magnitude and change in direction near 2103 may indicate passage of the sudden commencement front. The satellite was at $12 R_e$, -20° magnetic latitude and at 1000 Local Time. The field vector, between 2104 and 2107 UT was pointing toward the magnetopause; it was lying closer to the ecliptic plane than before the sudden commencement and was pointing east of the sun-earth line in a "garden hose" direction (Table 1). Note that the low energy protons and electrons rose somewhat earlier at 2100 (Hoffman et al, 1962).

Table 1

Time	B	Solar Ecliptic Latitude	Longitude
2100, 30 Sept.	40 γ	-30°	102°
2107 "	15 γ	18°	159°
2116 "	40 γ	13°	115°

By 2110 the magnitude had recovered to nearly 50 gammas and by 2115 the field direction had assumed a new direction about 40° from the old. Both before and after this event the field points nearly antiparallel to

the earth's field. On the time scale of these data samples, one point (10 second average) per minute, there is no indication of erratic or turbulent fields during storm front passage. The initial change in magnitude and direction took place in less than 1 minute (6×10^4 Km. thickness if the shock front velocity is 1000 Km/sec). The layer of field pointing toward the magnetopause took 5 to 10 minutes to pass.

The satellite continued outward to apogee during the initial phase of the storm. The next inbound pass, during the late main phase and early recovery phase is shown in Figure 4. The field magnitude is unusually high, 50 to 100 gammas, and several large changes in direction occur between 0300 and 0900 UT while the satellite is beyond the magnetopause. Between 0930 and 1000 UT the field direction becomes close to the dipole direction. Apparently the satellite has entered the magnetosphere although large fluctuations in direction and magnitude continue. At 1040 the field direction reverses. We interpret this as evidence that the magnetopause has been pushed in past the satellite. The magnetosphere is re-entered at 1100. As the satellite continues inward the fluctuations become smaller. Note that the measured field magnitude is considerably higher than predicted at $5 R_e$. Thus, during the early recovery phase of a great magnetic storm, there is no evidence of field depression between $5 R_e$ and the boundary. On the next outbound pass the magnetopause has expanded beyond apogee at $13 R_e$. The magnetopause is not penetrated again until 3 October.

Figure 5 shows a record of field magnitude obtained on the September 29 outbound pass during a quiet period before the storm. The orbit is plotted in the local geomagnetic meridian plane, with geomagnetic latitude and radial distance as the coordinates. The differences in field magnitude, measured minus predicted, are shown along the orbit as vertical lines.

The differences are small ($< 10\gamma$) from $L=5$ to $L = 8$. The measured field appears to be slightly lower than predicted from $L = 5$ to 7 but not significantly so in view of the estimated accuracy of the data. Figure 6 does show a definite field depression from $L = 3.5$ to $L = 6$. This pass was during the recovery phase of the storm of 24 September while Dst was still approximately -25γ . The depression in field magnitude observed at the satellite was greater than 20γ , $L = 3.5$ to 4.5. Note that the satellite trajectory crosses the magnetic equator at $L=6$ and remains below 10° magnetic latitude at $L = 3.5$. The magnetic records terminate at low altitude due to saturation of the magnetometer amplifiers as the main field increases above 1000γ .

Figure 7a is a composite record of the inbound passes during the main and recovery phases of the 30 September storm and Figure 7b contains the outbound records. We emphasize that this data was obtained principally during the recovery phase of a great magnetic storm. The outbound passes, from 3 to 8 R_e were near the 0900 local time meridian while the inbound passes were near 1100 local time. The first outbound record at the top of Figure 7b is immediately before the storm and shows compression near the boundary but small positive difference field at lower altitudes. The next, 1-2 October, is from the first outbound pass after the main phase. The difference is large and positive at 3 to 5 R_e ($L=4$ to 7), decreasing slowly in the outer portions of the orbit. The boundary is beyond apogee and the large 40γ differences near 4 R_e are obviously not due to compression. The trajectories of the last four outbound passes are, at low altitudes, in the same region of $R - \lambda$ space. The general features remain, large positive difference near 4 R_e , decreasing at greater distances. The differences on 5 October are somewhat less than

on 2 October but still greater than 30 gammas.

The top record of Figure 7a is for October 1 while the main phase is ending. The differences are great near the boundary but at $4 R_e$ they are only 15 to 20 gammas, considerably less than for 1 - 2 October outbound pass. The 2 October inbound pass shows differences greater than 20 gammas. The 3 October inbound differences are about 15 gammas and the 4 October differences, obtained at a slightly lower latitude, only a few gammas. The 5-6 October inbound record indicates small negative differences at $3 R_e$ while the outbound record from the same day shows 30 gamma positive differences. The boundary was at $10.5 R_e$ on 3 October inbound and at $11 R_e$ on 4 October inbound. Beyond these distances are transition region fields.

The principal features of these records are the large positive differences on the outbound passes and the smaller differences, becoming negative by 5 October, on the inbound passes. It is important to note that the outbound passes traverse increasingly greater magnetic latitudes (and higher L shells at the same radial distance) on successive days while the inbound passes are at progressively lower latitudes. It is also important that the magnitude of total vector distortion field is not obtained in the data presented. We have subtracted measured field magnitude from predicted field magnitude. Since the difference vector is of order 10 to 100 and the total field 500 to 1000 γ , the difference vector component parallel to the main field is selected by this procedure.

Discussion

The magnetosphere had recovered by 29 September from an earlier storm on 24 September. The 29 September outbound pass and the 30 September outbound pass in Figure 7b show that the field magnitude from $L=5$ to 7 is distorted very little, 0 to ± 10 gammas, from the predicted magnitude. During the storm sudden commencement and initial phase the magnetosphere must be compressed but since the satellite is beyond the magnetopause this cannot be confirmed. The magnetosheath (transition region) field is moderately high, 30 to 50 gammas, prior to the sudden commencement. The sudden impulse that occurred 2 hours earlier may have been related to the solar plasma stream that caused the storm.

The field change at 2103 UT was preceded at 2100 by appearance of electrons 10 to 35 kev, and a factor of 100 increase in protons, $E > 200$ kev. A slow rise, started at 2045 for the protons (Hoffman, et al, 1962). At 2030 protons, $E > 5$ Mev, started to rise (Bryant et al, 1962). All of this evidence supports the idea that the field change at 2103 indicates passage of the plasma front that caused the storm sudden commencement. The 6 minute delay, until 2109 when the sudden commencement was observed on earth, if considered as hydromagnetic wave propagation time implies an average HM velocity 200 km/sec. It is not certain whether the change indicates passage of the plasma front travelling through the magnetosheath or inward passage of the standing bow shock wave. The location of this event, at $12 R_e$, places it near the closest ($\sim 13 R_e$) shock front observation by Ness et al, 1964. The shock front, as well as the boundary, must move inward at sudden commencement. During the interval 2103 to 2110 UT, the satellite may have been in the interplanetary medium with the shock front then expanding outward past the satellite. It is possible that the field after 2110 is also interplanetary but

unusually high in magnitude. The approximate field directions in solar ecliptic coordinates at 2100, 2107 and 2116 were given in Table 1.

From 2120 to 2300 UT, 30 September, the initial phase continued. By 0000, 1 October, the main phase development had started; the greatest field depression occurred in the interval, 0200 to 1500 with the effects of large polar disturbances superimposed on the main phase depression on ground magnetograms. From 0900 to 1400, 1 October the storm rapid recovery proceeded while the satellite was inbound from $10 R_e$ to $3 R_e$ (Figure 4). This record is of great interest since the boundary location of $8.6 R_e$ shows that the solar wind pressure was still high during the rapid recovery phase. Fluctuations in pressure were producing large movements of the boundary on the sunlit side of the magnetosphere as late as 1100 UT. High magnetic field in the magnetosheath, 0300 to 0930 UT, indicates that the interplanetary field, as well as the solar wind pressure, was high and erratic during the main phase. Although large boundary motions apparently occur several times during this interval, we have been unable to identify the resultant sudden impulses on ground magnetograms. The search for ground level evidence is hampered by the large ionospheric effects caused by polar substorms. Soon after 1500, 1 October, during the recovery phase the boundary expanded past $13 R_e$. This behavior of the boundary, pushed close to the earth during the maximum depression of the main phase (minimum Dst) and expanding during the recovery phase has been observed for other storms and has been reported earlier (Freeman, 1964, Cahill and Patel, 1966).

These observations while the satellite was in the transition region, can reveal little of the development of the main phase deep in the magnetosphere; but during the longer slow recovery phase some useful conclusions can be obtained. It is particularly apparent in the outbound passes

of Figure 7b that, at magnetic latitudes greater than 30° and at L values above 5 the recovery phase of this storm is seen as an increase in field magnitude of 30 to 40 gammas. On the inbound passes, October 2 and 3, the distortion in magnitude at $\lambda_m \approx +30^\circ$, $L \approx 5$ is positive but somewhat less than seen on the outbound passes. The October 1 inbound pass also has a lower positive distortion. Since the rapid recovery phase is in progress this may be due to time and spatial variation in the main phase distortion. Later in the slow recovery phase the distortion is steady, decaying slowly and is expected, if due to trapped charged particles, to be approximately symmetrical about the magnetic dipole axis and about the magnetic equator. The discrepancy between the inbound and outbound passes at $4 R_e$ on 2 and 3 October may be due to error in measurement, to small differences in latitude or in L value (the October 2-3 outbound pass is at $L = 7$, $\lambda_m = -40^\circ$ at $4 R_e$ while 3 October inbound is at $L = 5$, $\lambda_m = +30^\circ$ at $4 R_e$), or to differences in local time.

The inner portions of the outbound passes are at progressively higher latitudes (-30° to -40°) and higher L shells while the inbound passes are at lower latitudes ($+30^\circ$ to $+15^\circ$) and lower L shells. The difference in field magnitude for the outbound passes remains positive and only slightly lower than 1-2 October pass at L values of 6 and above. The difference in field magnitude decreases for the lower L values and latitudes of the inbound passes. A negative magnitude difference is observed at $L = 3.5$ to 4.5 near $+15^\circ$ latitude on 6 October.

The large positive differences above $L = 5$ are interpreted as due to a belt of trapped particles on lower L shells. ($L = 2$ to $L = 5$). Such positive distortions are predicted by calculation of the magnetic fields due to trapped particle belts (Akasofu and Cain, 1962). The

negative differences seen at lower L values (Oct. 5-6 In) are interpreted as due to depression of the field within the ring current particle belt. Apparently the satellite has not reached the greatest field depression (at the maximum particle density). D_{st} on the earth's surface was approximately -20γ at this time. A similar or somewhat greater depression is expected at the center of the particle belt according to the model calculations, and after consideration of the contribution due to sub-surface currents.

Magnetometer data, not shown here, acquired just prior to saturation indicates that on the high latitude passes the positive field differences drop rapidly near $L = 5$. Although these data are less reliable, near saturation, they suggest entry of the satellite into the belt of trapped particles below $L = 5$, that is causing inflation of the magnetosphere. In comparing the satellite records with the results of Akasofu, et al, (1961, 1962) we see that there is qualitative agreement. The model difference field is positive beyond the particle belt and reaches the greatest negative value near the center of the belt intensity. There is a quantitative discrepancy, however. The maximum positive difference on October 5 outbound is about $+30 \gamma$ near $R = 4 R_e$ ($L = 7$), $\lambda_m = -40^\circ$. For October 5-6 inbound corresponding difference is only $+8 \gamma$ near $R = 7 R_e$ ($L = 7$), $\lambda_m = +7^\circ$. Figures 5 and 3 of Akasofu, et al, 1961, correspond roughly to these two passes. Comparison is difficult since the model belt of this calculation has its center at $6 R_e$ rather than at $3 R_e$. Still it is clear that this model does not predict a difference between F and F dipole outside the belt ($8 R_e$ in their Fig. 3, $5 R_e$ in their Fig. 5), that is greater at $\lambda_m = 40^\circ$ than at 10° . The pitch angle

distribution, $A(\alpha) \sin^{\alpha+1} \theta$, for this model has $\alpha = -\frac{1}{2}$, corresponding to a greater density of particles at small pitch angles than for an isotropic particle flux. It appears that, with such a model, a greater field distortion at high latitudes can be produced only by increasing the particle density there, by lowering α still more. The pitch angle distribution used by Akasofu et al, 1962, for the quiet time proton belt ($E > 100$ kev) has $\alpha = +2.0$. Hoffman and Bracken, 1965, use $\alpha = 2.5$.

In addition to the experimental errors discussed earlier in this paper there are several other difficulties in interpretation of this distortion data. The reference field magnitude, subtracted from measured field magnitude, may be inaccurate. Heppner et al, 1961, find discrepancies between the magnitudes of the measured field of the low altitude Vanguard 3 satellite and reference fields as great as 2% (Finch and Leaton, 1957; Jensen and Whitaker, 1960). The more recent reference field computed by Jensen and Cain, 1962 was used in this study, but great improvement in the reference field accuracy is not expected (Cain et al, 1962). The 2% discrepancies at low altitude may be distributed between the dipole term of the internal field and the higher multipoles. The main field above 3 Re is principally due to the dipole term and 2% can be taken as the maximum discrepancy, approximately 20 gammas at 3 Re and approximately 6 gammas at 5 Re. Errors in orbital position may be considered equivalent to reference field errors. The orbit of Explorer 12 was determined with high accuracy, however, after many orbits, and field errors from this source are believed to be much lower than the reference field errors.

Compression of the magnetosphere by the solar wind also produces a field distortion. Since the boundary is observed to be in frequent

motion, 8 to 13 Re during Explorer 12 lifetime, a variable distortion field due to boundary location is present at 3 to 8 Re. The boundary distance during the period 2 to 7 Oct. was observed to vary from 10 Re to greater than 13 Re. From boundary model results we estimate that the distortion contribution due to the boundary at 4 Re, on the equator, varied from 25 γ to 15 γ (Mead, 1964). At higher latitudes the boundary compression causes less increase in field magnitude; between 30° and 60° magnetic latitude, according to Mead, the boundary distortion reverses sign and decreases the field magnitude at higher latitudes.

Dolginov et al, 1966, find that the measured field magnitude is less than their predicted reference field magnitude below 5 Re on outward passes (geographic latitude less than 30°) and below 7 Re on inward passes (geographic latitude less than 60°). They observe depressions of field magnitude 50 to 100 γ near 3 Re on most passes. During storms the depressions, on occasion, reach several hundred gammas. These data were obtained in February-April 1964 while the Elektron 2 satellite orbit moved from the dawn meridian past the midnight meridian.

The Elektron 2 data appear to disagree with the Explorer 12 data; there are several possible reasons for the disagreement. Experimental errors are present in each set of data and are estimated to be less than 20 γ (Elektron 2) and 25 γ (Explorer 12). Different reference fields were used; it appears unlikely that this would cause more than 10 γ disagreement above 3 Re. The Explorer 12 data were obtained in 1961; the Elektron data were obtained in 1964 during lower solar and geomagnetic activity. The Elektron data cover 3 months with generally low magnetic activity although there were several small storms. The Explorer 12 data presented here was obtained during a large storm. Other data obtained

during quiet times do not show the consistent depression below 5 Re observed by Elektron 2. The effects of boundary compression have not been accounted for in either set of data. These effects are comparable to the observed field differences and vary between the noon and midnight meridians and at different latitudes. Mead, 1964, predicts a decrease in field magnitude due to boundary pressure at 60° magnetic latitude.

Frank, 1966, with a total energy detector on Explorer 12, observed large increases (to $1000 \text{ ergs cm}^{-2} \text{ sec}^{-1}$) in the flux of electrons, $100 \text{ ev} < E < 40 \text{ kev}$, during the development of the main phase of the magnetic storms, on 1 Oct. and 29 Oct., 1961. These transient (1 day) increases and enhancement above the prestorm level by a factor of two for several days after the 30 Sept. storm are observed from $L = 2.8$ to 4.0 with the greatest increase at $L = 3.0$. These electrons appear to constitute a portion of the particles that cause the storm time inflation of the magnetosphere. The total energy measurements do not rule out low energy protons as an additional contribution to the inflation.

Conclusions

The magnetosphere is inflated during the magnetic storm of 30 September, 1961. The inflating particles form a belt between $L = 2$ and $L = 5$ (Frank, 1966). The high latitude magnetic measurements of Explorer 12 are obtained outside this belt and an increase in field magnitude is observed. Low latitude measurements, within but not at the center of the belt, show a field depression. The Explorer 12 measurements are not necessarily in disagreement with Elektron 2 results. The magnetosphere distortion is the vector sum of boundary and ring current inflation fields, plus transient effects, and further progress demands precise vector treatment of the problem.

Acknowledgements

This work was supported by NASA Grants NsG-624 and NsG-538 and Contract NASw-155.

References

- Akasofu, S. I. , J. C. Cain, and S. Chapman, The magnetic field of a model radiation belt, numerically computed, J. Geophys. Research, 66, 4013-4026, 1961.
- Akasofu, S. I., and S. Chapman, The ring current, geomagnetic disturbance, and the Van Allen radiation belts, J. Geophys. Research, 66, 1321-1350, 1961.
- Akasofu, S. I., J. C. Cain, and S. Chapman, The magnetic field of the quiet-time proton belt, J. Geophys. Research, 67, 2645-2647, 1962.
- Akasofu, S. I., S. Chapman, and D. Venkatesan, The main phase of great magnetic storms, J. Geophys. Research, 68, 3345-3350, 1963.
- Akasofu, S. I., and J. C. Cain, The magnetic field of the radiation belts, J. Geophys. Research, 67, 4078-4080, 1962.
- Akasofu, S. I., The main phase of magnetic storms, and the ring current, Space Science Rev., 2, 91-135, 1963.
- Apel, J. R., S. F. Singer, and R. C. Wentworth, Effects of trapped particles on the geomagnetic field, Advances in Geophysics, 9, 131-189, 1962.
- Beard, D. B., Self-consistent calculation of the ring current, J. Geophys. Research, 67, 3615-3616, 1962.
- Bryant, D. A., T. L. Cline, U. D. Desai, and F. B. McDonald, Explorer 12 observations of solar cosmic rays and energetic storm particles after the solar flare of September 28, 1961, J. Geophys. Research, 67, 4983-5000, 1962.

References (Continued)

- Cahill, L. J., Inflation of the magnetosphere near 8 earth radii in the dark hemisphere, to be published in Space Research 6, Proc. 6th Int. Space Sci. Symp. Buenos Aires, 1965, Books Inc., Washington, D. C., 1966.
- Cahill, L. J., and P. G. Amazeen, The boundary of the geomagnetic field, J. Geophys. Research, 68, 1835-1843, 1963.
- Cahill, L. J. and D. H. Bailey, Distortions of the geomagnetic field within the inner-magnetosphere (abstract), Trans. A. G. U., 46, 116, 1965.
- Cahill, L. J. and V. L. Patel, The boundary of the geomagnetic field, August to November, 1961, U. N. H. Research Report 64-11, submitted to Planetary and Space Sci., May, 1966.
- Cain, J. C., I. R. Shapiro, J. D. Stolarik, and J. P. Heppner, Vanguard 3 magnetic-field observations, J. Geophys. Research, 67, 5055-5069, 1962.
- Chapman, S., and V. C. A. Ferraro, A new theory of magnetic storms, Terrest. Magnetism and Atmospheric Elec., 36, 77-97, 1931.
- Chapman, S., and V. C. A. Ferraro, A new theory of magnetic storms, II, The main phase, Terrest. Magnetism and Atmospheric Elec., 38, 79-96, 1933.
- Davis, L. R., and J. M. Williamson, Low energy trapped protons, in Space Research 3, Proc. 3rd Intern. Space Sci. Symp., Washington, 1962, North-Holland Publishing Company, Amsterdam, 1963.

References (Continued)

- Dessler, A. J., W. B. Hanson, and E. N. Parker, Formation of the geomagnetic storm main-phase ring current, J. Geophys. Research, 66, 3631-3637, 1961.
- Dessler, A. J., and E. N. Parker, Hydromagnetic theory of geomagnetic storms, J. Geophys. Research, 64, 2239-2252, 1959.
- Dolginov, Sh. Sh., E. G. Yeroshenko, L. N. Zhuzgov, N. V. Pushkov, and L. O. Tyurmina, Magnetic measurements with the Second Cosmic Rocket, Artificial Earth Satellites, Vols. 3, 4 and 5 (translated from Russian), edited by L. V. Kurnosova, Plenum Press, New York, pp. 490-502, 1961.
- Dolginov, Sh. Sh., E. G. Yeroshenko, and L. N. Zhuzgov, Investigation of the earth's magnetosphere in the region of the radiation belt (3-6 Re) from February to March 1964, to be published in Space Research 6, Proceedings of the 6th Int'l. Space Sci. Symp., Buenos Aires, 1965. Books Inc., Washington, D. C., 1966.
- Finch, H. F., and B. R. Leaton, The earth's main magnetic field - epoch 1955.0, Monthly Notices Roy. Astron. Soc. Geophys. Suppl., 7, 314-317, Nov. 1957.
- Frank, L. A., Explorer 12 observations of the temporal variations of low-energy electron intensities in the outer radiation zone during geomagnetic storms, U. of Iowa Report 66-8, March, 1966.

References (Continued)

- Freeman, J. W. Jr., The morphology of the electron distribution in the outer radiation zone and near the magnetospheric boundary as observed by Explorer 12, J. Geophys. Res., 1691-1724, 1964.
- Heppner, J. P., T. L. Skillman, and J. C. Cain, Contributions of rockets and satellites to the world magnetic survey, Space Research 2, Proc. 2nd Intern. Space Sci. Symp., Florence, 681-691, 1961.
- Heppner, J. P., N. F. Ness, C. S. Searce, and T. L. Skillman, Explorer 10 magnetic field measurements, J. Geophys. Research, 68, 1-46, 1963.
- Hoffman, R. A., and P. A. Bracken, Magnetic effects of the quiet-time proton belt, J. Geophys. Research, 70, 3541-3556, 1965.
- Hoffman, R. A., L. R. Davis, and J. M. Williamson, Protons of 0.1 to 5 Mev and electrons of 20 Kev at 12 earth radii during sudden commencement on September 30, 1961, J. Geophys. Research, 67, 5001-5005, 1962.
- Jensen, D. C., and J. C. Cain, An interim geomagnetic field (abstract), J. Geophys. Res., 67, 3568, 1962.
- Jensen, D. C., and W. A. Whitaker, A spherical harmonic analysis of the geomagnetic field (abstract), J. Geophys. Res., 65, 2500, 1960.
- Kern, J. W., A note on the generation of the main-phase ring current of a geomagnetic storm, J. Geophys. Research, 67, 3737-3751, 1962.
- Mead, G. D., Deformation of the geomagnetic field by the solar wind, J. Geophys. Res., 69, 1101-1195, 1964.

References (Continued)

- Ness, N. F., C. S. Scarce, and J. B. Seek, Initial results of the Imp 1 magnetic field experiment, J. Geophys. Research, 69, 3531-3569, 1964.
- Nishida, A., and L. J. Cahill, Sudden impulses in the magnetosphere observed by Explorer 12, J. Geophys. Research, 69, 2243-2255, 1964.
- Parker, E. N. Dynamics of the geomagnetic storm, Space Science Rev., 1, 62-99, 1962.
- Patel, V. L., and L. J. Cahill, The magnetic storm of September 30, 1961: Explorer 12 measurements (abstract), J. Geophys. Res. 67, 3585, 1962.
- Singer, S. F., A new model of magnetic storms and aurorae, Trans. Am. Geophys. Union, 38, 175-190, 1957.
- Smith, E. J., A comparison of Explorer VI and Explorer X magnetometer data, J. Geophys. Research, 67, 2045-2049, 1962.
- Van Allen, J. A., The geomagnetically trapped corpuscular radiation, J. Geophys. Research, 64, 1683-1689, 1959.

Figure Captions

- Figure 1 Dst index, 24 September through 10 October 1961. Midnight of each day is indicated by long tick mark, noon by short mark, on time scale. Plotted from Dst data on magnetic tape provided by W. Paulishak, Geomagnetism Div. Washington Science Center, ESSA.
- Figure 2 Record of 30 September Sent. 1961 outbound pass. Total field magnitude, $|B|$, scale in gammas, spacecraft direction angles α and ψ in degrees, and radial distance in earth radii. Universal time and magnetic latitude are shown at top.
- Figure 3 Detailed view of a segment of the 30 Sept. record. $|B|$, α and ψ scales are the same as in Figure 2. Scale at base is universal time of measurement.
- Figure 4 Record of 1 Oct. 1961 inbound pass. Scales are the same as in Figure 2.
- Figure 5 Difference in magnitude, on 29 Sept. outbound pass, between measured field and predicted (Jensen and Cain, 1962) field, $|B_{\text{meas}}| - |B_J \text{ and } C|$. Vertical lines denoting magnitude difference start at location of measurement in the magnetic meridian plane. Heavy curve shows orbit. End of lines, dotted, are above line for positive difference and below line for negative difference. Magnetic latitude lines and lines of constant L are shown. Radial distance in earth radii is indicated along equator.
- Figure 6 Difference in magnitude for 26-27 Sept. inbound pass.
- Figure 7 Summary of magnitude difference records for 30 September, 1961, magnetic storm. Figure 7a shows inbound passes; 7b shows outbound passes.

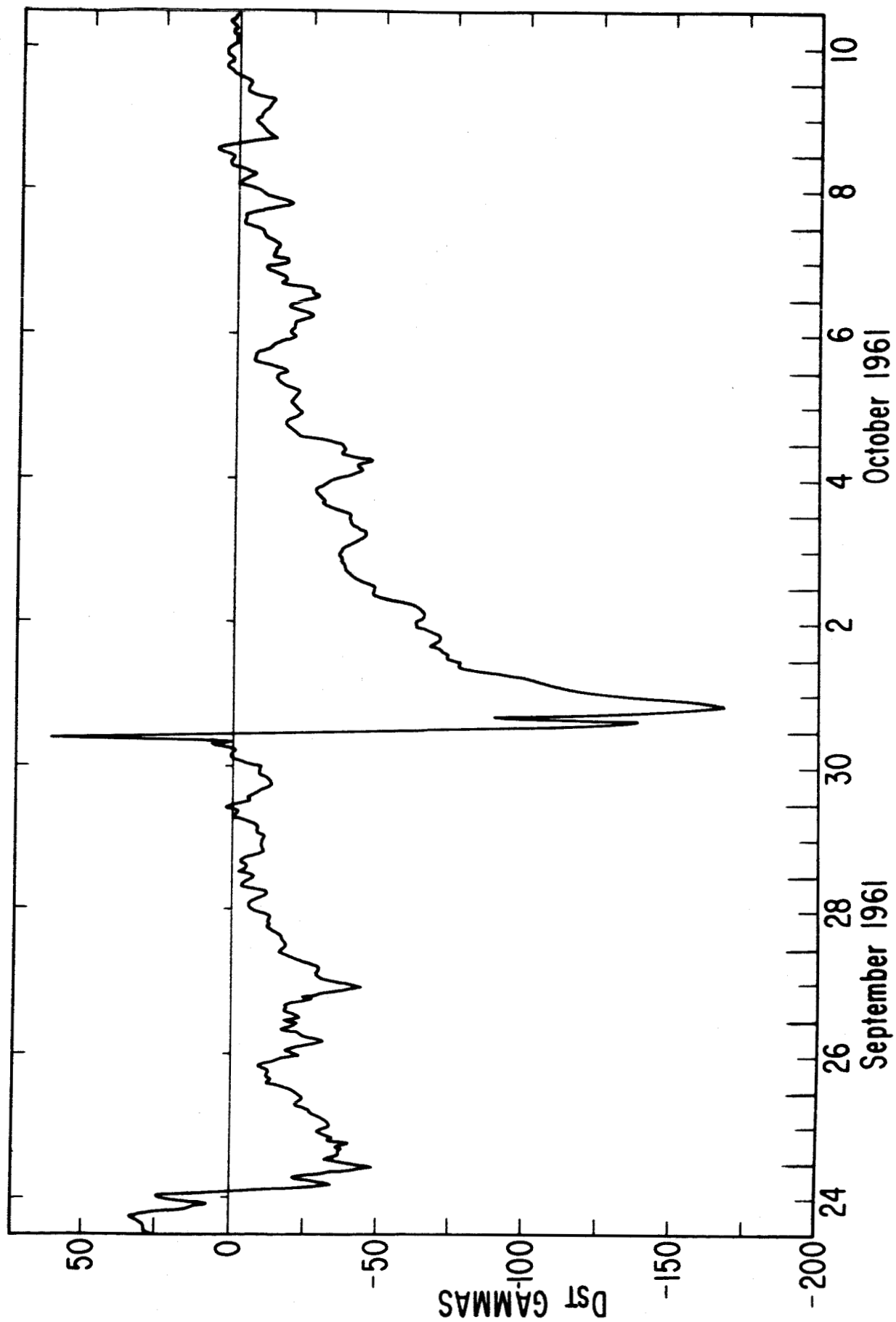


FIGURE 1

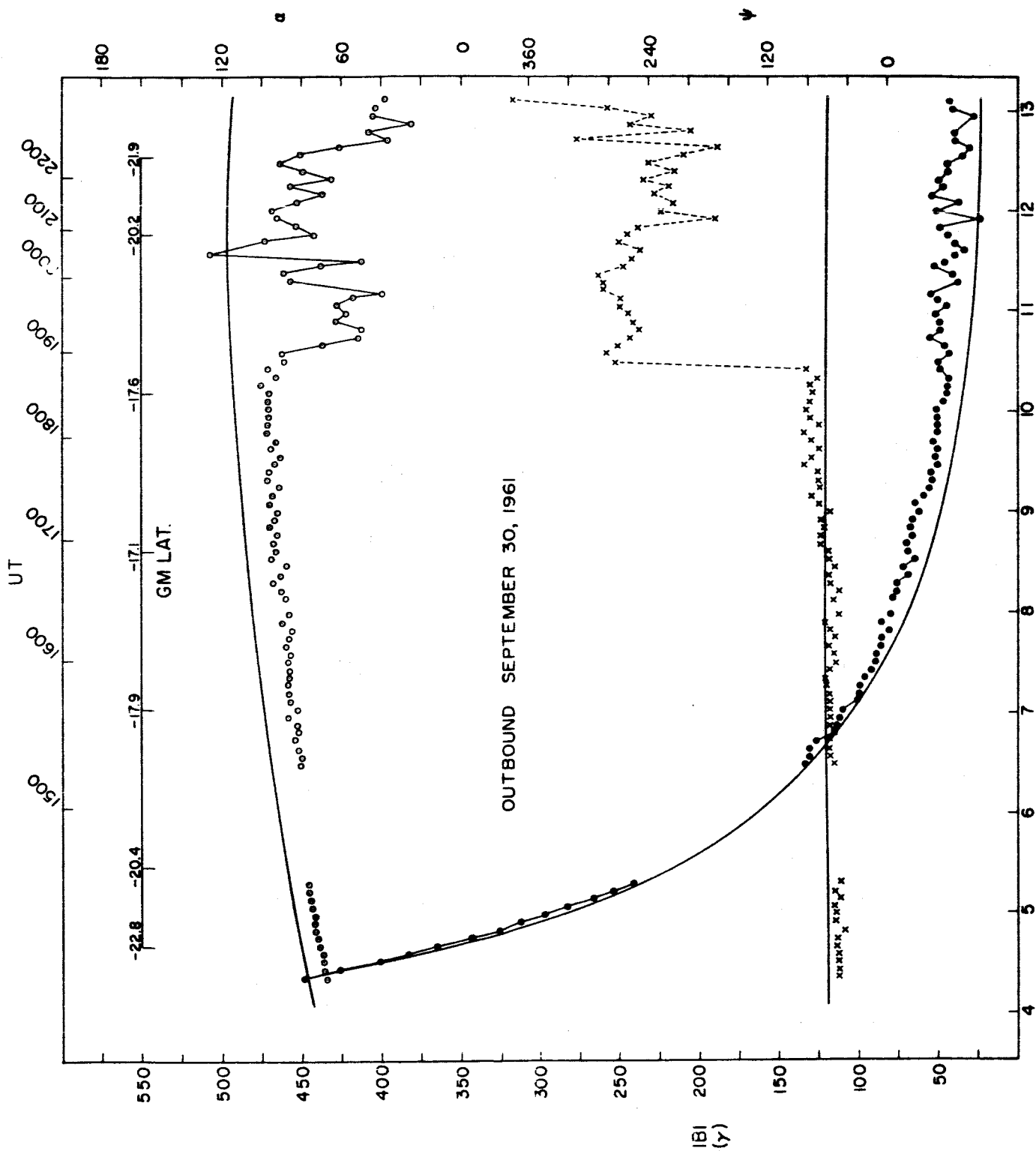


FIGURE 2

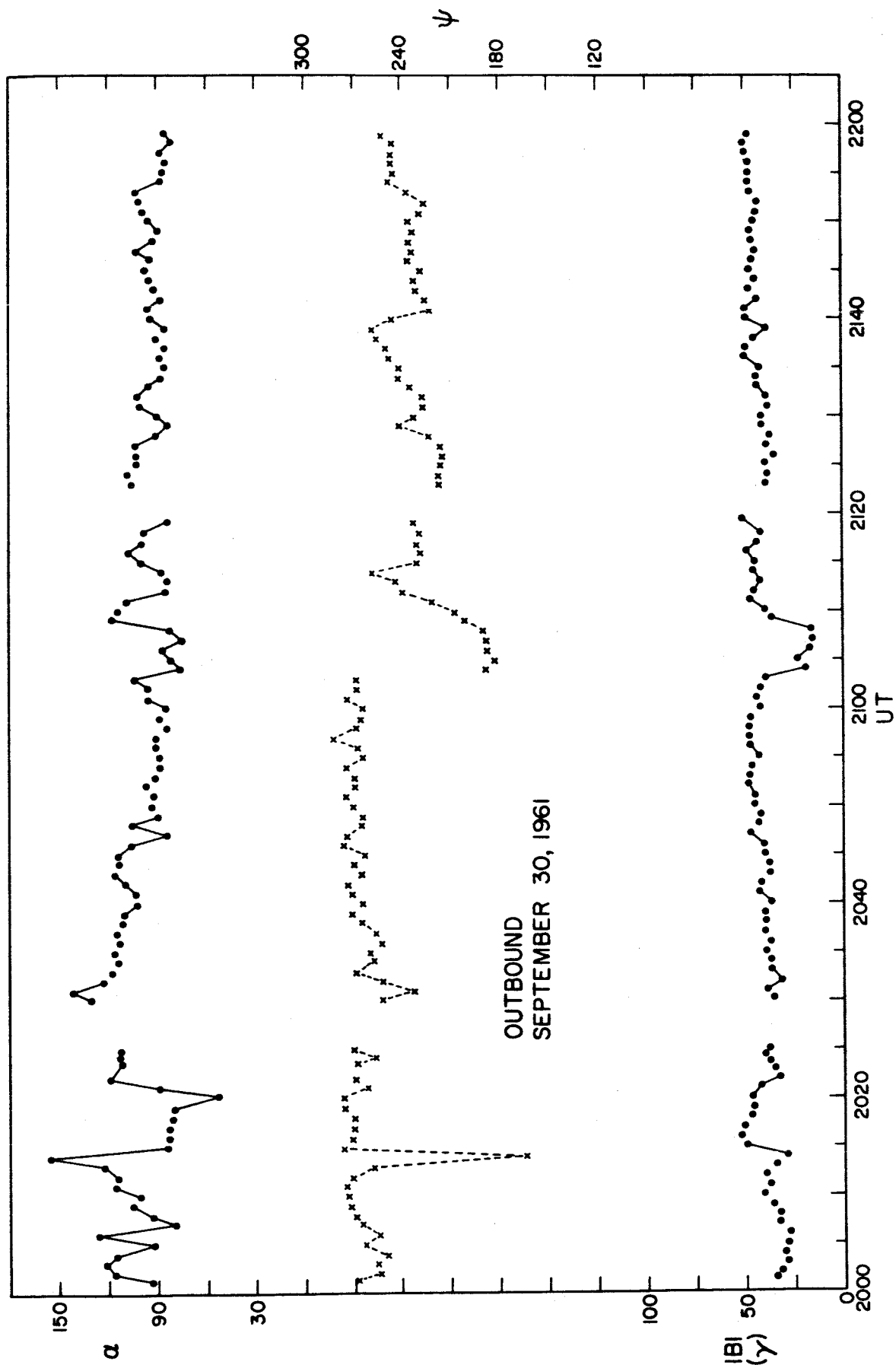


FIGURE 3

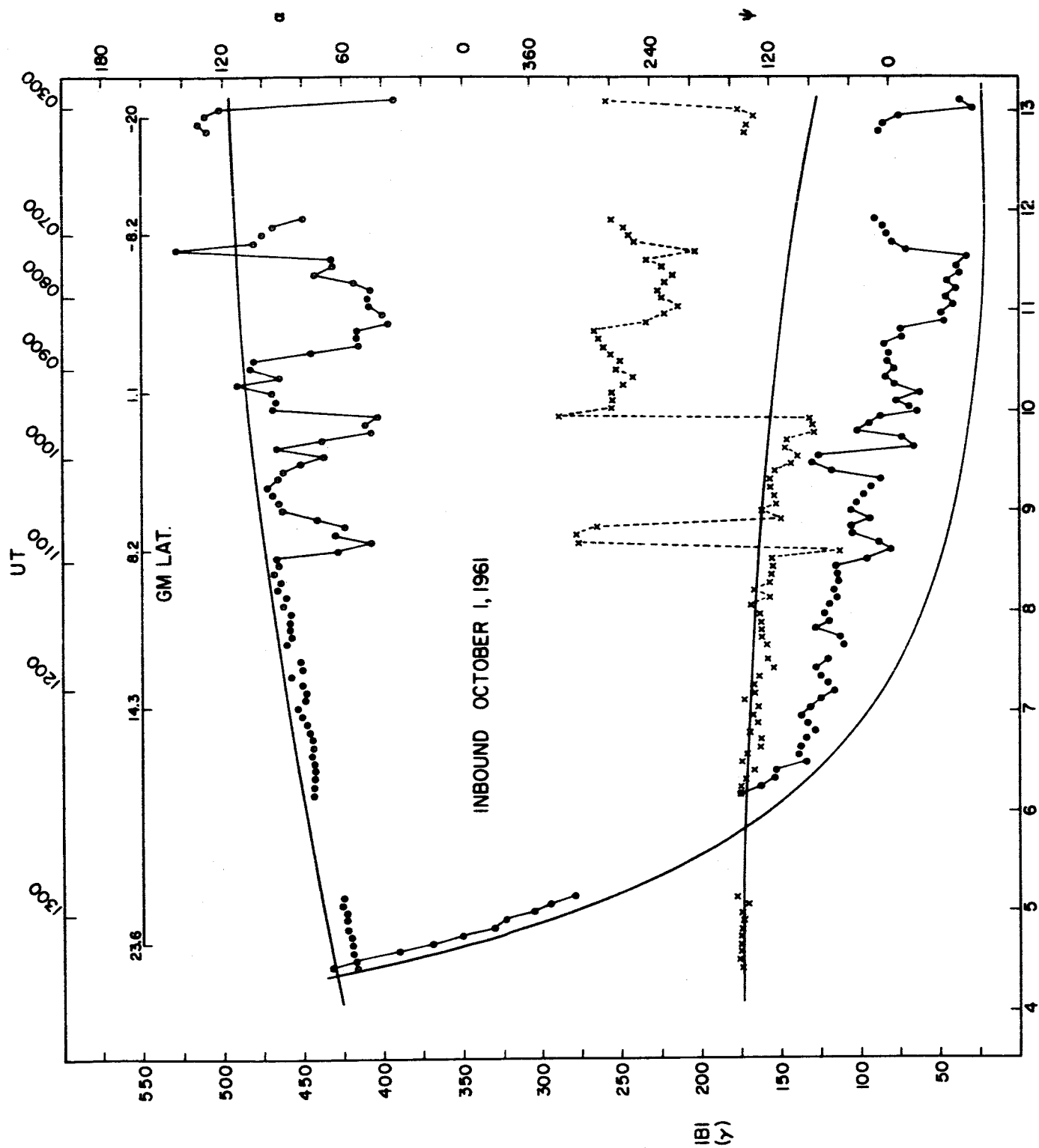


FIGURE 4

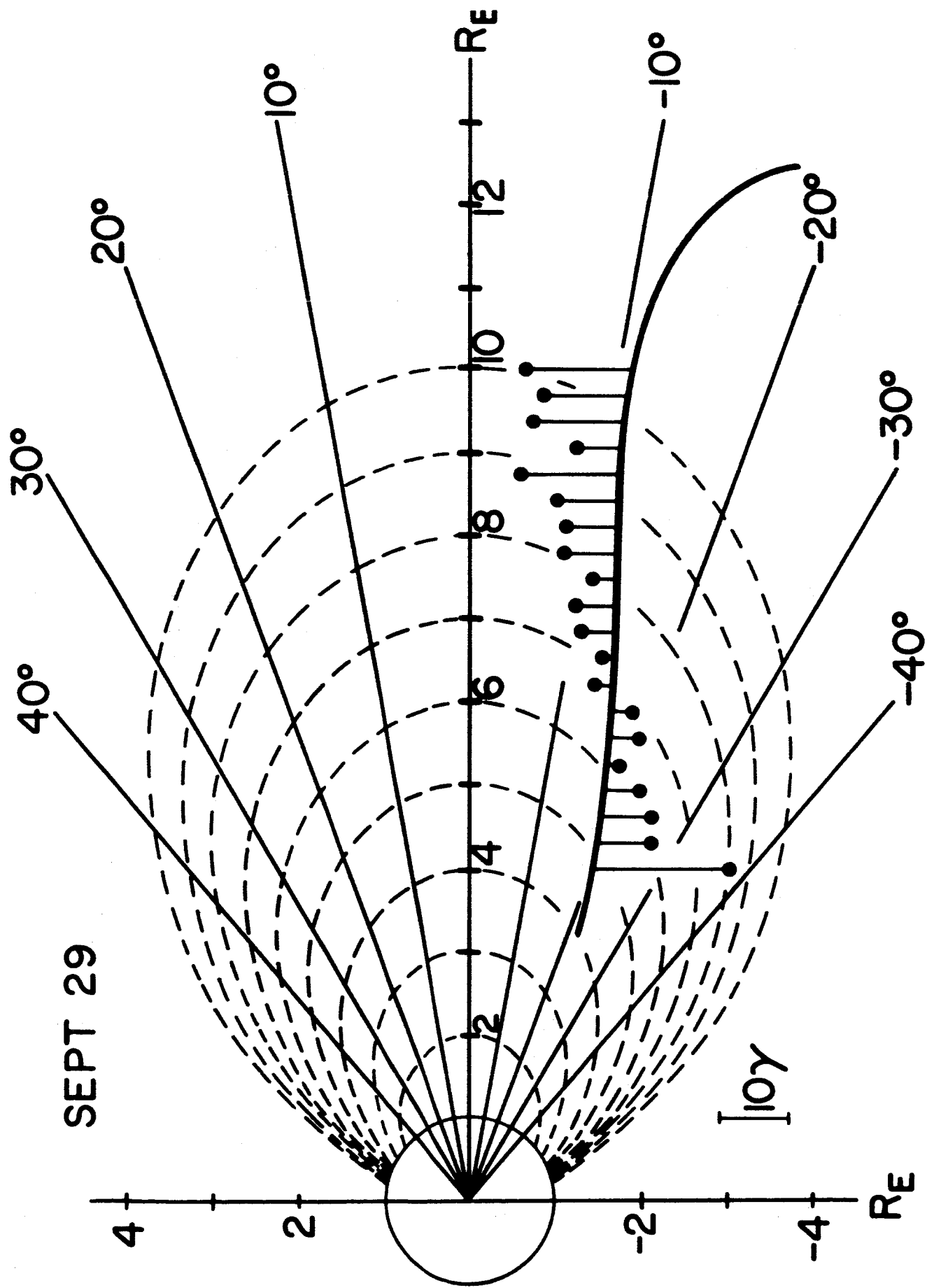


FIGURE 5

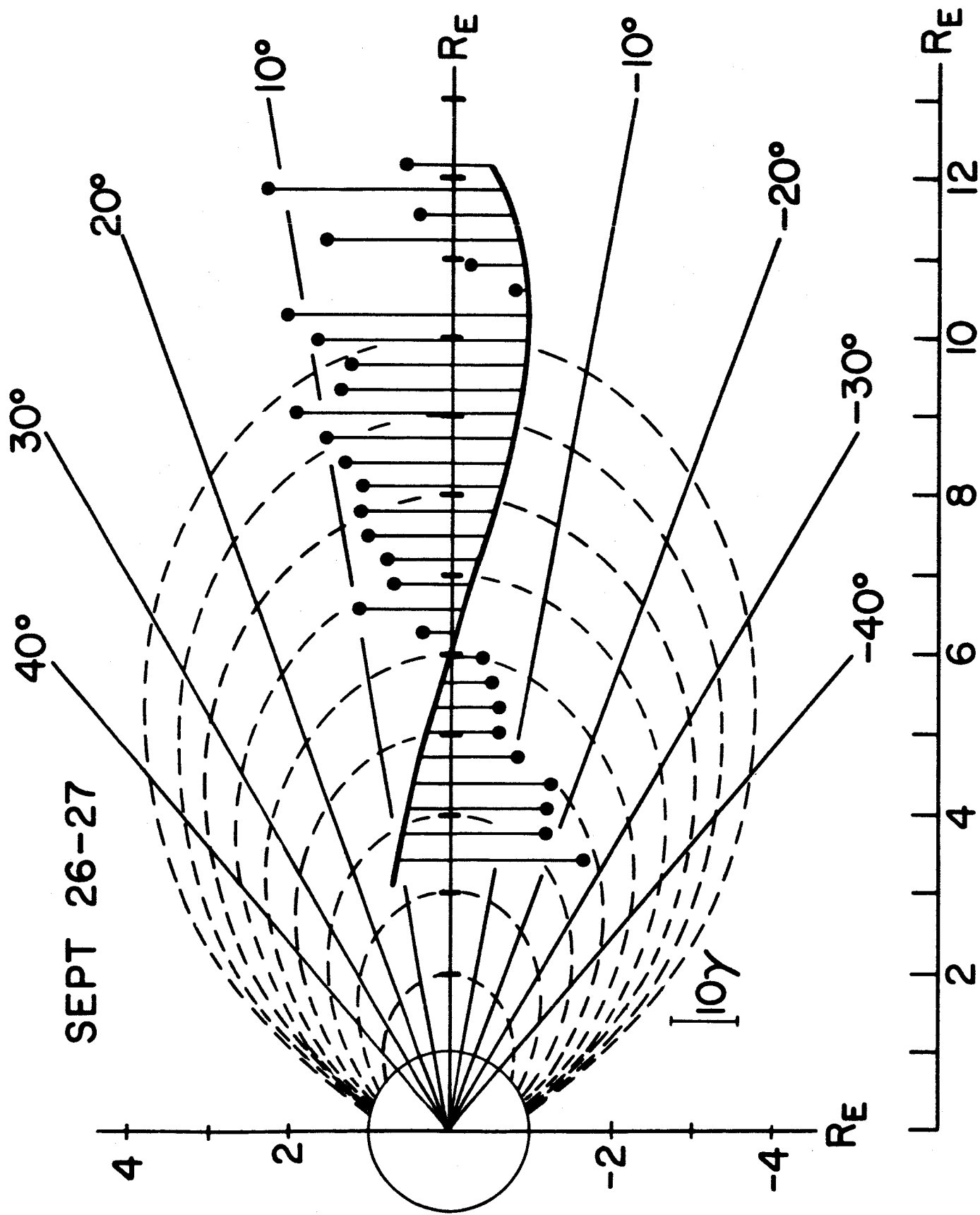


FIGURE 6

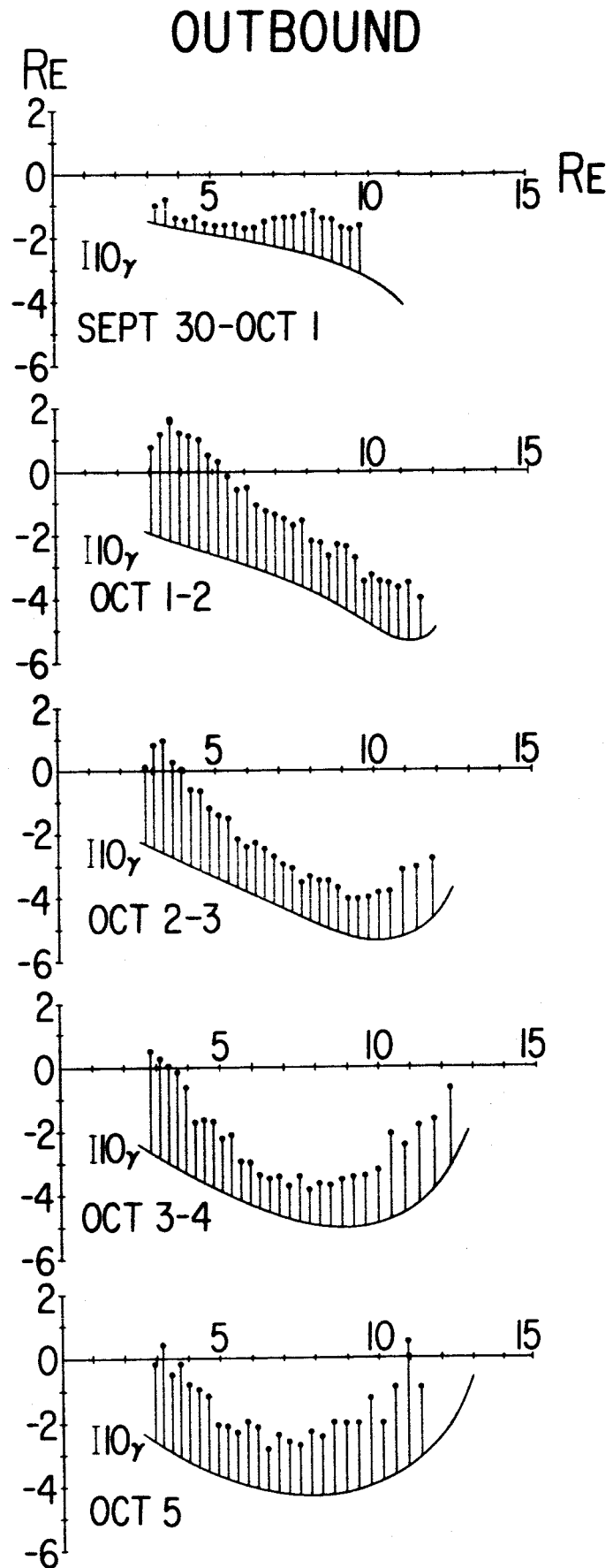
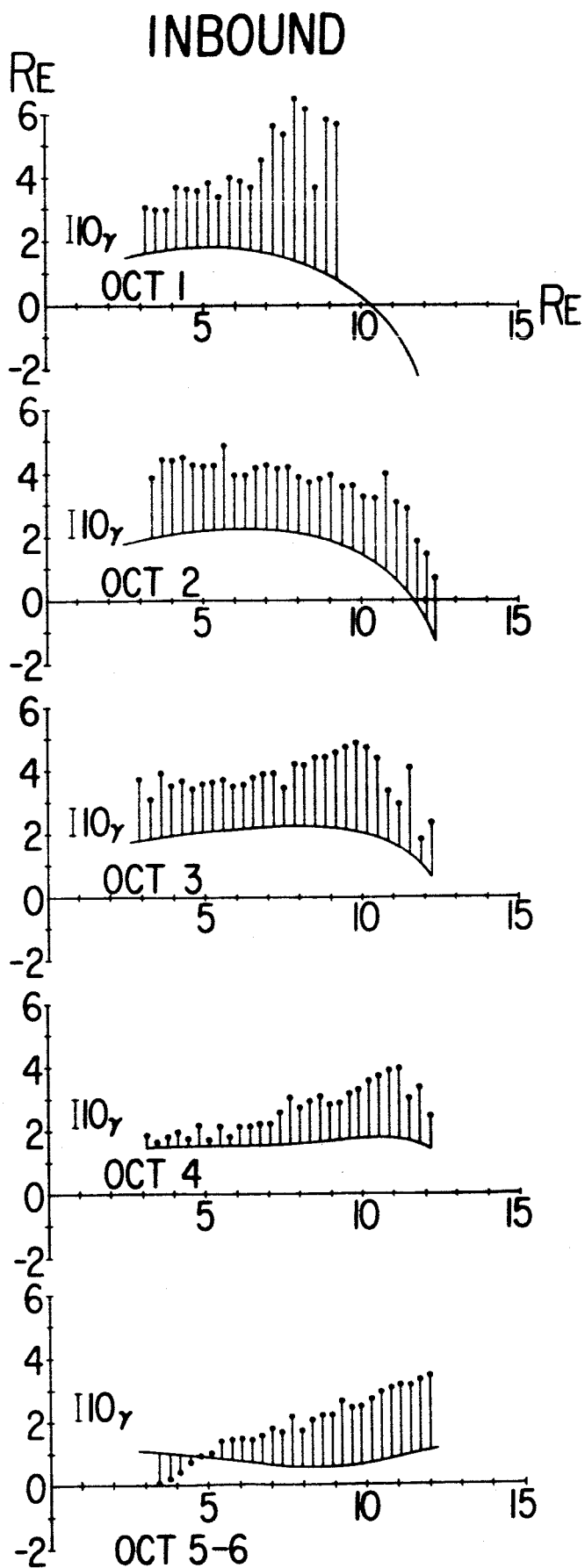


FIGURE 7